Photoacoustic Imaging Techniques

Subjects: Others

Contributor: Dong-Wook Han

2D materials can be used as carriers for delivering therapeutic agents into a lesion, leading to phototherapy. Various optical imaging techniques have been used for the monitoring of the treatment process.

Keywords: 2D materials ; phototherapy ; photoacoustic imaging ; image-guided therapy

1. Introduction

Two-dimensional nanomaterials with a well-ordered 2D planar structure (thickness > 100 nm) have been widely developed. Thanks to their beneficial biocompatible and biodegradable characteristics, various types of 2D nanomaterials, such as graphene derivatives; LDH, layered double hydroxide; TMD, transition metal dichalcogenide; TMO, transition metal oxide; and BP, black phosphorus, have been used for biomedical applications including drug delivery, tissue engineering, bio-imaging, and bio-sensing[1] (Figure 1). Because such materials have beneficial physicochemical properties of biocompatibility and degradability, they are suitable for biomedical applications including drug delivery, tissue engineering, bio-imaging, and biosensors[2][3][4][5][6]. Two-dimensional nanomaterials can cause a photothermal effect that generates heat by converting light energy into thermal energy when they are irradiated with near-infrared (NIR) light, and can then be used for phototherapy[7].

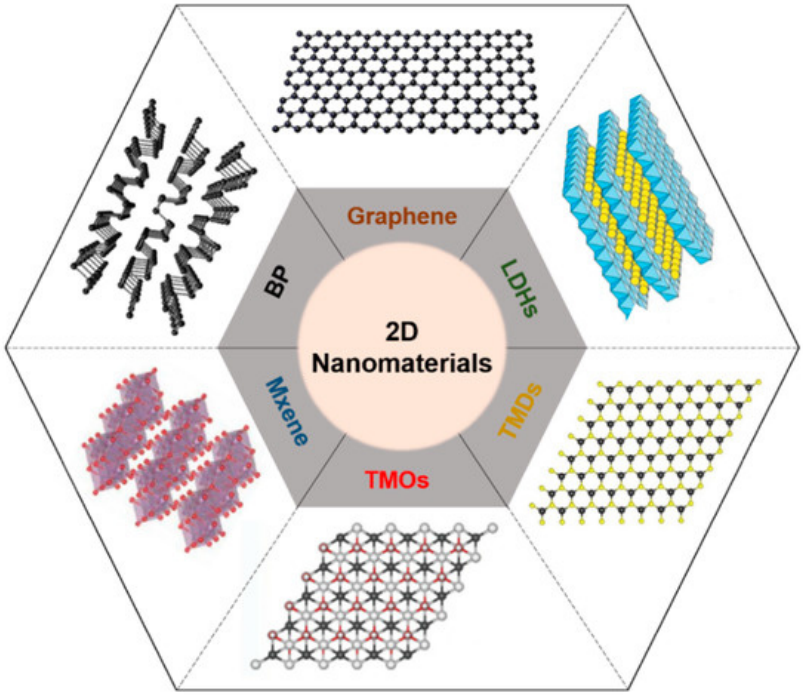

Figure 1. Schematic illustration of representative 2D nanomaterials. LDH, layered double hydroxide; TMD, transition metal dichalcogenide; TMO, transition metal oxide; BP, black phosphorus.

The representative phototherapy methods are photothermal therapy (PTT) and photodynamic therapy (PDT)[8]. In PTT, the local heating of NIR-absorbing agents is triggered by NIR light illumination. As tumor cells have difficulty dissipating heat, the NIR-triggered photothermal effect causes selective death of cancerous cells, which can be ablated more than 42 °C through necroptosis and apoptosis, which is programmed cell death, while endowing little damage to normal cells[9]. In contrast, PDT is an indirect method using photosensitizers that generate harmful singlet oxygen ($^1O_2$) when they absorb light. As PDT does not generate heat, nanomaterials in PDT usually perform as carriers that transfer photosensitizers using their surface properties[10]. To assess the therapy, drug delivery, and biodegradability, visualization of the internal biodistribution is essential.

Various biomedical imaging techniques, such as X-ray computed tomography (CT), magnetic resonance imaging (MRI), and positron emission tomography (PET), have been used for visualizing the distribution of nanomaterials, monitoring the delivery of nanomaterials, and assessing the efficacy of treatments[11][12][13][14]. Particularly, optical imaging techniques have been widely used as they provide high optical contrast, rich functional information, and excellent spatiotemporal resolution[15]. Compared with other biomedical imaging techniques, optical imaging systems can be implemented with low cost and simple configuration. In addition, optical imaging does not create harmful ionizing radiation, which makes the system favorable for future clinical translation. However, despite the advantages set out above, optical imaging is not widely used in clinics. The primary limitation of optical imaging is shallow imaging depth due to photon scattering in biological tissue[16].

Photoacoustic (PA) imaging is a biomedical imaging technique that combines the principles of ultrasound (US) and optical imaging[17]. The principle of PA imaging is based on the PA effect, which involves energy transduction from laser to acoustic waves through thermoelastic expansion (Figure 2). The typical procedure of PA imaging is as follows: (1) illumination of a short (typically a few nanoseconds) pulsed laser beam to target tissue, (2) light absorption and heat release by the optically absorbing chromophores, (3) acoustic wave (i.e., PA wave) generation through rapid thermal expansion and relaxation, (4) signal reception using US transducer, and (5) image generation and display. Because PA imaging inherits the principles of optical and US imaging techniques, it can provide both strong optical contrast and high ultrasound resolution in deep tissue[18][19]. In addition to intrinsic chromophores (oxy- and de-oxy-hemoglobins, melanin, lipids, and water), external agents (organic dyes, liposomal nanoformulations, nanoparticles, and nanostructures) have been widely used to obtain contrast-enhanced PA images[20][21][22][23]. Moreover, using multiple wavelengths of the excitation laser, molecular functional information of biological tissue can be obtained, which can be used for investigating the bio-distribution of external agents in vivo[24][25][26].

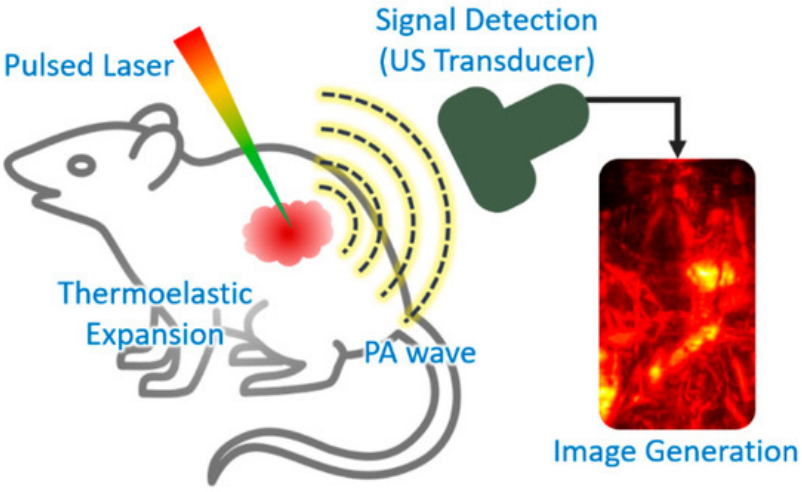

Figure 2. Schematic explanation of the procedure of PA imaging. PA, photoacoustic; US, ultrasound. The inset image is reproduced with permission from[27].

2. Phototherapy Using 2D Nanomaterials

2.1. Types and Characteristics

Currently, various phototherapy agents including gold nanostructures[28][29], mesoporous silica nanoparticles[30][31], and 2D nanomaterials have been widely investigated for clinical application. Among them, 2D nanomaterials are attracting the most attention because they can be used not only for phototherapy, but in other biomedical fields thanks to their excellent biochemical properties (Table 2). Typical 2D nanomaterials consist of one or a few atomic layers. As a representative 2D nanomaterial, graphene has a honeycomb structure consisting of carbon atoms. By changing the shape, the number of layers, and chemical modifications, several derivatives can be formed. Among them, graphene oxide (GO)[28] and reduced graphene oxide (rGO)[29][30] have been widely utilized for biomedical applications because of their superior electrical and thermal conductivities, large surface area, chemical versatility, and biocompatibility[31][32][33]. Layered double hydroxides (LDHs) are inorganic 2D nanomaterials with structures in which metal atoms are sandwiched by hydroxide layers. Because of their high charge density with excellent biocompatibility, LDHs are widely used as nano-carriers for theranostic agents in drug or gene delivery, phototherapy, and immunotherapy[34][35][36]. Transition metal dichalcogenides (TMDs) have hexagonal lattices consisting of monolayers of transition metal atoms between chalcogen atom layers. In addition to thin, flexible, and strong characteristics, TMDs are excellent optical absorbers, thus producing photolimunescence and photothermal effects [37][38][39][40]. TMDs can be formed with various materials including molybdenum disulfide (MoS_2)[41]

[42][43][44], tungsten disulfide (WS_2)[45][46][47][48], and molybdenum diselenide ($MoSe_2$)[49][50][51]. Transition metal oxides (TMOs) are compounds of oxygen atoms and transition metals such as titanium (TiO_2)[52][53] and manganese (MnO_2)[54][55][56]. Their wide bandgap results in excellent photochemical and electric properties[57][58]. They can also directly interact with drugs, genes, or other biomolecules by surface modification and thus can be utilized in biomedical applications including drug delivery, cancer therapy, tissue engineering, bio-imaging, and biosensing[59][60][61]. Mxenes are the most recently discovered 2D materials and have been applied in various biomedical applications because of their extreme thinness, large surface area, high surface–volume ratio, and mechanical strength[62][63][64][65][66]. Black phosphoruses (BP) are the most stable allotropes of phosphorus with zigzag or armchair bilayer structures. BP have shown potential in biomedical applications with their strong optical absorption in the ultraviolet (UV) and NIR regions [67][68][69][70][71]. They have also demonstrated promising biocompatibility and biodegradation[72].

2.2. Phototherapy Using 2D Nanomaterials

By taking advantage of their strong optical absorption and thermal transition properties, 2D nanomaterials have been used for PTT. Liu et al. successfully prepared a doxorubicin (DOX)-loaded MoS_2-PEG nanosheet for combined PTT–chemo cancer therapy[73]. In that study, nanosheets were analyzed for drug delivery and photothermal effects by NIR irradiation. MoS_2-PEG/DOX nanosheets exhibited synergistic anti-cancer effects, inhibiting tumor growth in in vivo experiments. Zeng et al. reported on ultrathin MnO_2 nanosheets of polyethylene glycol-cyclic arginine-glycineaspartic acid tripeptide (PEG-cRGD) and encapsulated chlorin e6 (Ce6) for PTT/PDT synergistic cancer therapy (Figure 5)[74]. In that study, the nanosheets showed photothermal efficiency of 39% and could be reduced by overexpressed acidic H_2O_2, which could efficiently generate O_2 and further enhance the therapeutic efficiency of PDT. Moreover, the MnO_2-PEG-cRGD/Ce6 exhibited pH-controlled and NIR-induced Ce6 release, and showed favorable therapeutic outcomes under a single 660 nm NIR laser.

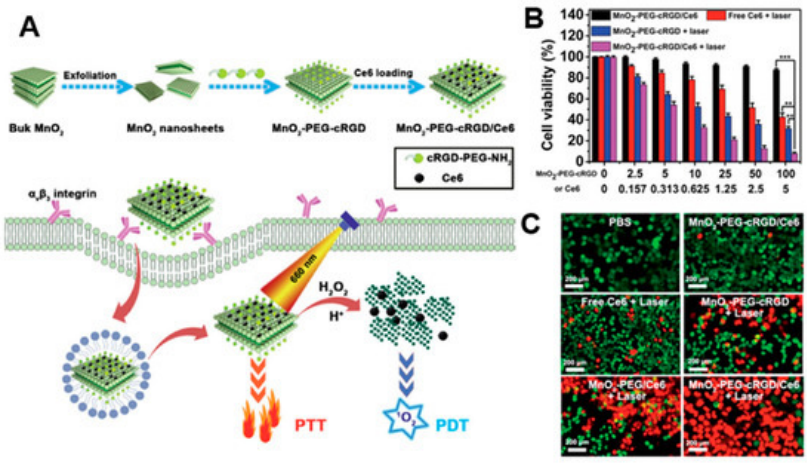

Figure 5. (**A**) Schematic illustration for the preparation of MnO_2-PEG-cRGD/Ce6 for synergistic photothermal/photodynamic (PTT/PDT) therapy. (**B**) Relative viabilities of PC3 cells after incubation with free Ce6, MnO_2-PEG-cRGD with 660 nm light irradiation, or MnO_2-PEG-cRGD/Ce6 with or without 660 nm light irradiation (0.6 W cm^{-2}, 10 min, *** $p < 0.001$, ** $p < 0.01$). (**C**) Fluorescence images of calcein acetoxymethyl ester (Calcein-AM, green)/propidium iodide (PI, red) double stained cells after different treatments. The images are reproduced with permission from[74].

A number of PDT studies have investigated the development of 2D nanomaterials that release photosensitizers. Moosavi et al. prepared N-TiO_2 nanoparticles to generate reactive oxygen species (ROS) and induce autophagy [52]. They showed the dose-dependent capability of well-dispersed photo-activated N-TiO_2 NPs to induce terminal megakaryocyte differentiation and cell death in K562 leukemia cells. In cellular experiments, N-TiO_2 nanoparticles increased ROS levels with light irradiation. Yang et al. fabricated covalently, incorporating both chlorin e6 (Ce6) and triphenyl phosphonium (TPP) onto BP@PDA NSs for dual-modal imaging-guided synergistic photothermal and photodynamic therapy (Figure 6) [75]. BP@PDA–Ce6&TPP NSs can produce considerable heat, mainly owing to BP@PDA NSs, and can generate sufficient ROS for PDT. With these results, BP@PDA–Ce6&TPP NSs can be used for PTT/PDT therapy of cancers.

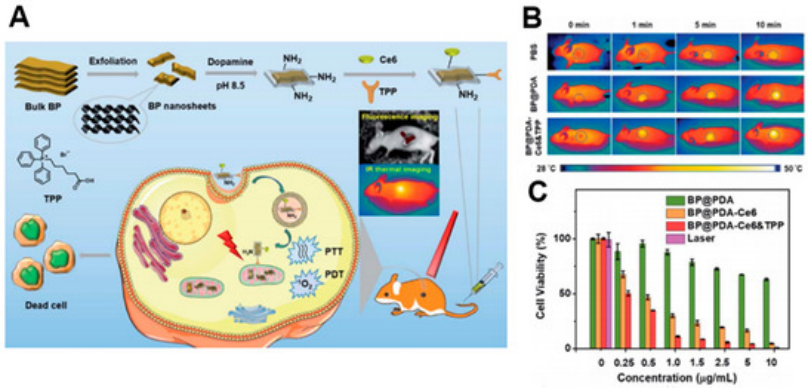

Figure 6. (**A**) Schematic illustrations of the preparation, therapeutic uses, and peaks in functions of BP@PDA–Ce6&TPP NSs. (**B**) Ex vivo fluorescence imaging of main organs as well as tumor at 24 h post-injection. (**C**) Relative viabilities of HeLa cells incubated with BP@PDA NSs, BP@PDA–Ce6 NSs, and BP@PDA–Ce6&TPP NSs at different BP@PDA concentrations with laser illumination (660 nm, 0.5 W cm^{-2}, 5 min). Data represent mean ± SD (n = 4). The images are reproduced with permission from[75].

Table 2. Phototherapy using 2D nanomaterials. PTT, photothermal therapy; PDT, photodynamic therapy.

2D Nanomaterials	Photothermal Conversion	Therapy	Applied Forms	Ref.
Graphene derivatives	63% (G), 35% (GO) [30]	PTT, PDT	GO-UCNPs-ZnPc	[32]
		PTT	GO/$MnFe_2O_4$/DOX	[33]
TiO_2	40.8% [57]	PTT	Ag@TiO_2	[53]
		PDT	N-TiO_2	[52]
MoS_2	0.84% [38]	PTT	MoS_2-HA-DTPA-Gd	[42]
		PTT, PDT	AuNBPs@MoS_2	[43]
		PTT	MoS_2-Gd-BSA	[44]
BP	30.84% [68]	PTT	BP-Au NSs	[69]
		PTT	BP-PEG-FA/Cy7 NSs	[70]
		PTT, PDT	BP@PEG/Ce6 NSs	[71]
Mxene(Ti_3C_2)	≒100% [63]	PTT	Ti_3C_2@Au	[64]
		PTT, PDT	Ti_3C_2-SP	[65]
		PTT, PDT	Ti_3C_2-DOX	[66]
WS_2	35% [39]	PTT, PDT	BSA-WS_2@MB	[46]
		PTT	WS_2-PEG	[47]
		PTT	WS_2-IO/S@MO-PEG	[48]
$MoSe_2$	54.3% [40]	PTT, PDT	$MoSe_2$/Fe_3O_4	[50]
		PTT, PDT	$MoSe_2$@PEG-Dox	[51]
2D Boron	42.5% [75]	PTT, PDT	B@Ce6–PAH–PAA	
MnO_2	62.4% [58]	PTT	MnO_2-PEG-FA/DOX	[55]
		PTT	BSA-MnO_2 NPs	[56]

References

1. Cao, X.; Halder, A.; Tang, Y.; Hou, C.; Wang, H.; Duus, J.Ø.; Chi, Q. Engineering two-dimensional layered nanomaterials for wearable biomedical sensors and power devices. Mater. Chem. Front. 2018, 2, 1944–1986.

2. Hu, T.; Mei, X.; Wang, Y.; Weng, X.; Liang, R.; Wei, M. Two-dimensional nanomaterials: Fascinating materials in biomedical field. Sci. Bull. 2019, 64, 1707–1727.
3. Guan, G.; Han, M.Y. Functionalized Hybridization of 2D Nanomaterials. Adv. Sci. 2019, 6, 1901837.
4. Yang, F.; Song, P.; Ruan, M.; Xu, W. Recent progress in two-dimensional nanomaterials: Synthesis, engineering, and applications. FlatChem 2019, 18, 100133.
5. Fusco, L.; Gazzi, A.; Peng, G.; Shin, Y.; Vranic, S.; Bedognetti, D.; Vitale, F.; Yilmazer, A.; Feng, X.; Fadeel, B. Graphene and other 2D materials: A multidisciplinary analysis to uncover the hidden potential as cancer theranostics. Theranostics 2020, 10, 5435.
6. Chimene, D.; Alge, D.L.; Gaharwar, A.K. Two-dimensional nanomaterials for biomedical applications: Emerging trends and future prospects. Adv. Mater. 2015, 27, 7261–7284.
7. Sundaram, P.; Abrahamse, H. Phototherapy Combined with Carbon Nanomaterials (1D and 2D) and their Applications in Cancer Therapy. Mater. Chem. Front. 2020, 13, 4830.
8. Lin, C.; Hao, H.; Mei, L.; Wu, M. Metal-free two-dimensional nanomaterial-mediated photothermal tumor therapy. Smart Mater. Med. 2020, 1, 150–167.
9. Liu, S.; Pan, X.; Liu, H. Two-Dimensional Nanomaterials for Photothermal Therapy. Angew. Chem. 2020, 132, 5943–5953.
10. Gazzi, A.; Fusco, L.; Khan, A.; Bedognetti, D.; Zavan, B.; Vitale, F.; Yilmazer, A.; Delogu, L.G. Photodynamic therapy based on graphene and MXene in cancer theranostics. Front. Bioeng. Biotechnol. 2019, 7, 295.
11. Ritman, E.L. Current status of developments and applications of micro-CT. Annu. Rev. Biomed. Eng. 2011, 13, 531–552.
12. Judenhofer, M.S.; Cherry, S.R. Applications for preclinical PET/MRI. In Seminars in Nuclear Medicine; Elsevier: Amsterdam, The Netherlands, 2013.
13. Xie, T.; Zaidi, H. Development of computational small animal models and their applications in preclinical imaging and therapy research. Med. Phys. 2016, 43, 111–131.
14. Wehrl, H.F.; Wiehr, S.; Divine, M.R.; Gatidis, S.; Gullberg, G.T.; Maier, F.C.; Rolle, A.-M.; Schwenck, J.; Thaiss, W.M.; Pichler, B.J. Preclinical and translational PET/MR imaging. J. Nucl. Med. 2014, 55, 11S–18S.
15. Pirovano, G.; Roberts, S.; Kossatz, S.; Reiner, T. Optical imaging modalities: Principles and applications in preclinical research and clinical settings. J. Nucl. Med. 2020, 61, 1419–1427.
16. Grashin, P.S.; Karabutov, A.A.; Oraevsky, A.A.; Pelivanov, I.M.; Podymova, N.B.; Savateeva, E.V.; Solomatin, V.S. Distribution of the laser radiation intensity in turbid media: Monte Carlo simulations, theoretical analysis, and results of optoacoustic measurements. Quantum Electron. 2002, 32, 868.
17. Bell, A.G. The photophone. Science 1880, 1, 130–131.
18. Kim, C.; Favazza, C.; Wang, L.V. In Vivo Photoacoustic Tomography of Chemicals: High-Resolution Functional and Molecular Optical Imaging at New Depths. Chem. Rev. 2010, 110, 2756–2782.
19. Kim, J.; Lee, D.; Jung, U.; Kim, C. Photoacoustic imaging platforms for multimodal imaging. Ultrasonography 2015, 34, 88.
20. Kim, J.; Park, S.; Lee, C.; Kim, J.Y.; Kim, C. Organic Nanostructures for Photoacoustic Imaging. ChemNanoMat 2015, 2, 156–166.
21. Lee, C.; Kim, J.; Zhang, Y.; Jeon, M.; Liu, C.; Song, L.; Lovell, J.F.; Kim, C. Dual-color photoacoustic lymph node imaging using nanoformulated naphthalocyanines. Biomaterials 2015, 73, 142–148.
22. Jeon, M.; Song, W.; Huynh, E.; Kim, J.; Kim, J.; Helfield, B.L.; Leung, B.Y.; Goertz, D.E.; Zheng, G.; Oh, J. Methylene blue microbubbles as a model dual-modality contrast agent for ultrasound and activatable photoacoustic imaging. J. Biomed. Opt. 2014, 19, 016005.
23. Park, S.; Kim, J.; Jeon, M.; Song, J.; Kim, C. In Vivo Photoacoustic and Fluorescence Cystography Using Clinically Relevant Dual Modal Indocyanine Green. Sensors 2014, 14, 19660–19668.
24. Lee, M.Y.; Lee, C.; Jung, H.S.; Jeon, M.; Kim, K.S.; Yun, S.H.; Kim, C.; Hahn, S.K. Biodegradable Photonic Melanoidin for Theranostic Applications. ACS Nano 2015, 10, 822–831.
25. De La Zerda, A.; Zavaleta, C.; Keren, S.; Vaithilingam, S.; Bodapati, S.; Liu, Z.; Levi, J.; Smith, B.R.; Ma, T.-J.; Oralkan, O. Carbon nanotubes as photoacoustic molecular imaging agents in living mice. Nat. Nanotechnol. 2008, 3, 557–562.
26. Zhang, Y.; Jeon, M.; Rich, L.J.; Hong, H.; Geng, J.; Zhang, Y.; Shi, S.; Barnhart, T.E.; Alexandridis, P.; Huizinga, J.D. Non-Invasive Multimodal Functional Imaging of the Intestine with Frozen Micellar Naphthalocyanines. Nat.

Nanotechnol. 2014, 9, 631–638.

27. Kim, J.; Park, S.; Jung, Y.; Chang, S.; Park, J.; Zhang, Y.; Lovell, J.F.; Kim, C. Programmable Real-time Clinical Photoacoustic and Ultrasound Imaging System. Sci. Rep. 2016, 6, 35137.
28. Lin, J.; Huang, Y.; Huang, P. Graphene-based nanomaterials in bioimaging. In Biomedical Applications of Functionalized Nanomaterials; Elsevier: Amsterdam, The Netherlands, 2018; pp. 247–287.
29. Tang, Y.; Zhao, Z.; Hu, H.; Liu, Y.; Wang, X.; Zhou, S.; Qiu, J. Highly stretchable and ultrasensitive strain sensor based on reduced graphene oxide microtubes–elastomer composite. ACS Appl. Mater. Interfaces 2015, 7, 27432–27439.
30. Savchuk, O.A.; Carvajal, J.; Massons, J.; Aguiló, M.; Díaz, F. Determination of photothermal conversion efficiency of graphene and graphene oxide through an integrating sphere method. Carbon 2016, 103, 134–141.
31. Zhu, X.; Liu, Y.; Li, P.; Nie, Z.; Li, J. Applications of graphene and its derivatives in intracellular biosensing and bioimaging. Analyst 2016, 141, 4541–4553.
32. Wang, Y.; Wang, H.; Liu, D.; Song, S.; Wang, X.; Zhang, H. Graphene oxide covalently grafted upconversion nanoparticles for combined NIR mediated imaging and photothermal/photodynamic cancer therapy. Biomaterials 2013, 34, 7715–7724.
33. Yang, Y.; Shi, H.; Wang, Y.; Shi, B.; Guo, L.; Wu, D.; Yang, S.; Wu, H. Graphene oxide/manganese ferrite nanohybrids for magnetic resonance imaging, photothermal therapy and drug delivery. J. Biomater. Appl. 2016, 30, 810–822.
34. Rives, V.; del Arco, M.; Martín, C. Intercalation of drugs in layered double hydroxides and their controlled release: A review. Appl. Clay Sci. 2014, 88, 239–269.
35. Khan, S.B.; Alamry, K.A.; Alyahyawi, N.A.; Asiri, A.M.; Arshad, M.N.; Marwani, H.M. Nanohybrid based on antibiotic encapsulated layered double hydroxide as a drug delivery system. Appl. Biochem. Biotechnol. 2015, 175, 1412–1428.
36. Bi, X.; Fan, T.; Zhang, H. Novel morphology-controlled hierarchical core@ shell structural organo-layered double hydroxides magnetic nanovehicles for drug release. ACS Appl. Mater. Interfaces 2014, 6, 20498–20509.
37. Liu, P.; Xiang, B. 2D hetero-structures based on transition metal dichalcogenides: Fabrication, properties and applications. Sci. Bull. 2017, 62, 1148–1161.
38. Fu, C.; Tan, L.; Ren, X.; Wu, Q.; Shao, H.; Ren, J.; Zhao, Y.; Meng, X. Interlayer expansion of 2D MoS2 nanosheets for highly improved photothermal therapy of tumors in vitro and in vivo. Chem. Commun. 2018, 54, 13989–13992.
39. Cui, X.-Z.; Zhou, Z.-G.; Yang, Y.; Wei, J.; Wang, J.; Wang, M.-W.; Yang, H.; Zhang, Y.-J.; Yang, S.-P. PEGylated WS2 nanosheets for X-ray computed tomography imaging and photothermal therapy. Chin. Chem. Lett. 2015, 26, 749–754.
40. He, L.; Nie, T.; Xia, X.; Liu, T.; Huang, Y.; Wang, X.; Chen, T. Designing Bioinspired 2D MoSe2 Nanosheet for Efficient Photothermal-Triggered Cancer Immunotherapy with Reprogramming Tumor-Associated Macrophages. Adv. Funct. Mater. 2019, 29, 1901240.
41. Pumera, M.; Loo, A.H. Layered transition-metal dichalcogenides (MoS2 and WS2) for sensing and biosensing. Trac Trends Anal. Chem. 2014, 61, 49–53.
42. Liu, J.; Zheng, J.; Nie, H.; Zhang, D.; Cao, D.; Xing, Z.; Li, B.; Jia, L. Molybdenum disulfide-based hyaluronic acid-guided multifunctional theranostic nanoplatform for magnetic resonance imaging and synergetic chemo-photothermal therapy. J. Colloid Interface Sci. 2019, 548, 131–144.
43. Maji, S.K.; Yu, S.; Chung, K.; Sekkarapatti Ramasamy, M.; Lim, J.W.; Wang, J.; Lee, H.; Kim, D.H. Synergistic Nanozymetic Activity of Hybrid Gold Bipyramid–Molybdenum Disulfide Core@ Shell Nanostructures for Two-Photon Imaging and Anticancer Therapy. ACS Appl. Mater. Interfaces 2018, 10, 42068–42076.
44. Chen, L.; Zhou, X.; Nie, W.; Feng, W.; Zhang, Q.; Wang, W.; Zhang, Y.; Chen, Z.; Huang, P.; He, C. Marriage of Albumin–Gadolinium Complexes and MoS2 Nanoflakes as Cancer Theranostics for Dual-Modality Magnetic Resonance/Photoacoustic Imaging and Photothermal Therapy. ACS Appl. Mater. Interfaces 2017, 9, 17786–17798.
45. Chia, X.; Eng, A.Y.S.; Ambrosi, A.; Tan, S.M.; Pumera, M. Electrochemistry of nanostructured layered transition-metal dichalcogenides. Chem. Rev. 2015, 115, 11941–11966.
46. Yong, Y.; Zhou, L.; Gu, Z.; Yan, L.; Tian, G.; Zheng, X.; Liu, X.; Zhang, X.; Shi, J.; Cong, W. WS2 nanosheet as a new photosensitizer carrier for combined photodynamic and photothermal therapy of cancer cells. Nanoscale 2014, 6, 10394–10403.
47. Cheng, L.; Liu, J.; Gu, X.; Gong, H.; Shi, X.; Liu, T.; Wang, C.; Wang, X.; Liu, G.; Xing, H. PEGylated WS2 nanosheets as a multifunctional theranostic agent for in vivo dual-modal CT/photoacoustic imaging guided photothermal therapy. Adv. Mater. 2014, 26, 1886–1893.
48. Yang, G.; Zhang, R.; Liang, C.; Zhao, H.; Yi, X.; Shen, S.; Yang, K.; Cheng, L.; Liu, Z. Manganese Dioxide Coated WS2@ Fe3O4/sSiO2 Nanocomposites for pH-Responsive MR Imaging and Oxygen-Elevated Synergetic

Therapy. Small 2018, 14, 1702664.

49. Zhou, X.; Sun, H.; Bai, X. Two-Dimensional Transition Metal Dichalcogenides: Synthesis, Biomedical Applications and Biosafety Evaluation. Front. Bioeng. Biotechnol. 2020, 8, 8.
50. Wang, Y.; Zhang, F.; Lin, H.; Qu, F. Biodegradable Hollow MoSe2/Fe3O4 Nanospheres as the Photodynamic Therapy-Enhanced Agent for Multimode CT/MR/IR Imaging and Synergistic Antitumor Therapy. ACS Appl. Mater. Interfaces 2019, 11, 43964–43975.
51. Wang, Y.; Zhang, F.; Wang, Q.; Yang, P.; Lin, H.; Qu, F. Hierarchical MoSe2 nanoflowers as novel nanocarriers for NIR-light-mediated synergistic photo-thermal/dynamic and chemo-therapy. Nanoscale 2018, 10, 14534–14545.
52. Moosavi, M.A.; Sharifi, M.; Ghafary, S.M.; Mohammadalipour, Z.; Khataee, A.; Rahmati, M.; Hajjaran, S.; Łos, M.J.; Klonisch, T.; Ghavami, S. Photodynamic N-TiO 2 nanoparticle treatment induces controlled ROS-mediated autophagy and terminal differentiation of leukemia cells. Sci. Rep. 2016, 6, 1–16.
53. Nie, C.; Du, P.; Zhao, H.; Xie, H.; Li, Y.; Yao, L.; Shi, Y.; Hu, L.; Si, S.; Zhang, M. Ag@ TiO2 Nanoprisms with Highly Efficient Near-Infrared Photothermal Conversion for Melanoma Therapy. Chem. Asian J. 2020, 15, 148–155.
54. Chen, Y.; Ye, D.; Wu, M.; Chen, H.; Zhang, L.; Shi, J.; Wang, L. Break-up of Two-Dimensional MnO2 Nanosheets Promotes Ultrasensitive pH-Triggered Theranostics of Cancer. Adv. Mater. 2014, 26, 7019–7026.
55. Hao, Y.; Wang, L.; Zhang, B.; Zhao, H.; Niu, M.; Hu, Y.; Zheng, C.; Zhang, H.; Chang, J.; Zhang, Z. Multifunctional nanosheets based on folic acid modified manganese oxide for tumor-targeting theranostic application. Nanotechnology 2015, 27, 025101.
56. Wang, Y.; Song, Y.; Zhu, G.; Zhang, D.; Liu, X. Highly biocompatible BSA-MnO2 nanoparticles as an efficient near-infrared photothermal agent for cancer therapy. Chin. Chem. Lett. 2018, 29, 1685–1688.
57. Li, W.; Elzatahry, A.; Aldhayan, D.; Zhao, D. Core–shell structured titanium dioxide nanomaterials for solar energy utilization. Chem. Soc. Rev. 2018, 47, 8203–8237.
58. Wang, L.; Guan, S.; Weng, Y.; Xu, S.-M.; Lu, H.; Meng, X.; Zhou, S. Highly efficient vacancy-driven photothermal therapy mediated by ultrathin MnO2 nanosheets. ACS Appl. Mater. Interfaces 2019, 11, 6267–6275.
59. Ma, R.; Sasaki, T. Nanosheets of oxides and hydroxides: Ultimate 2D charge-bearing functional crystallites. Adv. Mater. 2010, 22, 5082–5104.
60. Kalantar-zadeh, K.; Ou, J.Z.; Daeneke, T.; Mitchell, A.; Sasaki, T.; Fuhrer, M.S. Two dimensional and layered transition metal oxides. Appl. Mater. Today 2016, 5, 73–89.
61. Azadmanjiri, J.; Kumar, P.; Srivastava, V.K.; Sofer, Z. Surface Functionalization of 2D Transition Metal Oxides and Dichalcogenides via Covalent and Non-covalent Bonding for Sustainable Energy and Biomedical Applications. ACS Appl. Nano Mater. 2020, 3, 3116–3143.
62. Lin, H.; Wang, X.; Yu, L.; Chen, Y.; Shi, J. Two-dimensional ultrathin MXene ceramic nanosheets for photothermal conversion. Nano Lett. 2017, 17, 384–391.
63. Li, R.; Zhang, L.; Shi, L.; Wang, P. MXene Ti3C2: An effective 2D light-to-heat conversion material. ACS Nano 2017, 11, 3752–3759.
64. Tang, W.; Dong, Z.; Zhang, R.; Yi, X.; Yang, K.; Jin, M.; Yuan, C.; Xiao, Z.; Liu, Z.; Cheng, L. Multifunctional two-dimensional core–shell mxene@ gold nanocomposites for enhanced photo–radio combined therapy in the second biological window. ACS Nano 2018, 13, 284–294.
65. Han, X.; Huang, J.; Lin, H.; Wang, Z.; Li, P.; Chen, Y. 2D ultrathin MXene-based drug-delivery nanoplatform for synergistic photothermal ablation and chemotherapy of cancer. Adv. Healthc. Mater. 2018, 7, 1701394.
66. Liu, G.; Zou, J.; Tang, Q.; Yang, X.; Zhang, Y.; Zhang, Q.; Huang, W.; Chen, P.; Shao, J.; Dong, X. Surface modified Ti3C2 MXene nanosheets for tumor targeting photothermal/photodynamic/chemo synergistic therapy. ACS Appl. Mater. Interfaces 2017, 9, 40077–40086.
67. Choi, J.R.; Yong, K.W.; Choi, J.Y.; Nilghaz, A.; Lin, Y.; Xu, J.; Lu, X. Black phosphorus and its biomedical applications. Theranostics 2018, 8, 1005.
68. Xu, D.; Liu, J.; Wang, Y.; Jian, Y.; Wu, W.; Lv, R. Black Phosphorus Nanosheet with High Thermal Conversion Efficiency for Photodynamic/Photothermal/Immunotherapy. ACS Biomater. Sci. Eng. 2020, 6, 4940–4948.
69. Yang, G.; Liu, Z.; Li, Y.; Hou, Y.; Fei, X.; Su, C.; Wang, S.; Zhuang, Z.; Guo, Z. Facile synthesis of black phosphorus–Au nanocomposites for enhanced photothermal cancer therapy and surface-enhanced Raman scattering analysis. Biomater. Sci. 2017, 5, 2048–2055.
70. Tao, W.; Zhu, X.; Yu, X.; Zeng, X.; Xiao, Q.; Zhang, X.; Ji, X.; Wang, X.; Shi, J.; Zhang, H. Black phosphorus nanosheets as a robust delivery platform for cancer theranostics. Adv. Mater. 2017, 29, 1603276.

71. Yang, X.; Wang, D.; Shi, Y.; Zou, J.; Zhao, Q.; Zhang, Q.; Huang, W.; Shao, J.; Xie, X.; Dong, X. Black phosphorus nanosheets immobilizing Ce6 for imaging-guided photothermal/photodynamic cancer therapy. ACS Appl. Mater. Interfaces 2018, 10, 12431–12440.
72. Xiong, S.; Chen, X.; Liu, Y.; Fan, T.; Wang, Q.; Zhang, H.; Chen, T. Black phosphorus as a versatile nanoplatform: From unique properties to biomedical applications. J. Innov. Opt. Health Sci. 2020.
73. Liu, T.; Wang, C.; Gu, X.; Gong, H.; Cheng, L.; Shi, X.; Feng, L.; Sun, B.; Liu, Z. Drug delivery with PEGylated MoS2 nano-sheets for combined photothermal and chemotherapy of cancer. Adv. Mater. 2014, 26, 3433–3440.
74. Zeng, D.; Wang, L.; Tian, L.; Zhao, S.; Zhang, X.; Li, H. Synergistic photothermal/photodynamic suppression of prostatic carcinoma by targeted biodegradable MnO2 nanosheets. Drug Deliv. 2019, 26, 661–672.
75. Ji, X.; Kong, N.; Wang, J.; Li, W.; Xiao, Y.; Gan, S.T.; Zhang, Y.; Li, Y.; Song, X.; Xiong, Q. A novel top-down synthesis of ultrathin 2D boron nanosheets for multimodal imaging-guided cancer therapy. Adv. Mater. 2018, 30, 1803031.